Available online at www.sciencedirect.com
ScienceDirect
Journal of Solid State Chemistry 179 (2006) 3664–3671
JOURNAL OF SOLID STATE CHEMISTRY
www.elsevier.com/locate/jssc

Synthesis and crystal structure of three silver indium double phosphates

M.A. Strelkov*, M.G. Zhizhin, L.N. Komissarova

Inorganic Chemistry Division, Department of Chemistry, Moscow State University, 119899 Moscow, Russia

Received 15 December 2005; received in revised form 28 July 2006; accepted 30 July 2006
Available online 10 August 2006

Abstract

Three new silver indium double phosphates $Ag_3In(PO_4)_2$ (I), β-(II) and α-$Ag_3In_2(PO_4)_3$ (III) were synthesized by solid state method (I and II—700 °C, III—900 °C). Compounds I and II crystallize into a monoclinic system (I—sp. gr. $C2/m$, $Z = 2$, $a = 8.7037(1)$Å, $b = 5.4884(1)$Å, $c = 7.3404(1)$Å, $\beta = 93.897(1)°$; II—sp. gr. $C2/c$, $Z = 4$, $a = 12.6305(1)$Å, $b = 12.8549(1)$Å, $c = 6.5989(1)$Å, $\beta = 113.842(1)°$), and compound III crystallize into a hexagonal system (sp. gr. R-3c, $Z = 6$, $a = 8.9943(1)$Å, $c = 22.7134(1)$Å). Their crystal structures were determined by the Rietveld analysis (I—$R_p = 6.47$, $R_{wp} = 8.54$; II—$R_p = 5.67$, $R_{wp} = 6.40$; III—$R_p = 7.30$, $R_{wp} = 9.91$). Structure of $Ag_3In(PO_4)_2$ is related to the sodium chromate structure type and is isotypic to α-$Na_3In(PO_4)_2$. The polymorphous modifications of β- and α-$Ag_3In_2(PO_4)_3$ are isostructural to sodium analogs (β- and α-$Na_3In_2(PO_4)_3$) and are related to alluaudite (II) and NASICON (III) structure types. Compounds I and II are not stable at temperature above 850 °C. $Ag_3In(PO_4)_2$ is decomposed providing silver orthophosphate Ag_3PO_4 and α-$Ag_3In_2(PO_4)_2$. β-$Ag_3In_2(PO_4)_3$ is transformed to α-$Ag_3In_2(PO_4)_3$.

Keywords: Double phosphates; Indium; Silver; X-ray diffraction; Rietveld analysis; NASICON-type structure; Alluaudite-type structure

1. Introduction

In present time investigators are interesting double phosphates of mono- and trivalent cations compositions $M^I_3M^{III}(PO_4)_2$ and $M^I_3M^{III}_2(PO_4)_3$. These compounds are related to different structure classis and have different properties, such as ionic conductivity and non-linear optic properties [1,2].

Compounds with formula $M^I_3M^{III}(PO_4)_2$ (M^I = Na, K; M^{III} = Y, Sc, In, Fe, rare earth elements) [3–8] crystallize in arcanite, glazerite and sodium chromate structural types. It is assumed that the ratio between the radii of the cations is the governing factor responsible for the formation of glaserite- or arcanite-like structures. The glaserite-like structures are stable for compounds in which the difference between the radii of the M^I and M^{III} cations [$\Delta r(M^I - M^{III})$] occupying the M, X and Y positions is in the range $0.59 \leqslant \Delta r(M^I - M^{III}) \leqslant 0.89$ Å. However, compounds that are characterized by $\Delta r(M^I - M^{III}) < 0.59$ Å and have glaserite-like structures are also known. Thus, $\Delta r(M^I - M^{III})$ for $Na_3Fe(PO_4)_2$ (glaserite structural type) is 0.38 Å. At $\Delta r(M^I - M^{III}) < 0.59$ Å, compounds generally crystallize in the arcanite structural type. The majority of representatives of the $M_3M^{III}(PO_4)_2$ group have structures of arcanite (β-K_2SO_4) or structures of an intermediate type (combinations of the β-K_2SO_4 and Na_2CrO_4 structures). In particular, the former structural type is typical of $K_3M^{III}(PO_4)_2$ (M^{III} = La–Yb) and the latter type is characteristic of $K_3In(PO_4)_2$ and β-$Na_3M^{III}(PO_4)_2$ (M^{III} = La–Lu, In). These compounds belong to arcanite-like phosphates.

Compounds with formula $M^I_3M^{III}_2(PO_4)_3$ (M^I = Li, Na; M^{III} = Sc, In, Fe) [9–18] crystallizing in NASICON and alluaudite structural type are formed by small trivalent cations.

$Na_3Sc_2(PO_4)_3$ is the most interesting compound [1]. It has ionic conductivity (high-temperature modification) and ferroelectric properties (low temperature modification).

There is few information about double phosphates with silver, although silver radius is closed to sodium radius ($\mathbf{r}_{Ag(VI)} = 1.15$ Å, $\mathbf{r}_{Na(VI)} = 1.02$ Å [19]). It is data concerning $Ag_3Sc_2(PO_4)_3$ [20] and compound with another compositions $AgCaIn_2(PO_4)_3$ [21]. The first phosphate

---

*Corresponding author. Fax: +7 95 932 8846.
E-mail address: maksimstr@newmail.ru (M.A. Strelkov).

0022-4596/$ - see front matter © 2006 Elsevier Inc. All rights reserved.
doi:10.1016/j.jssc.2006.07.044

has NASICON-like structure and the second one has alluaudite-like structure.

Information about silver and indium phosphates $Ag_3In(PO_4)_2$ and $Ag_3In_2(PO_4)_3$ is absent in the literature. And in this work, we describe synthesis and crystal structure of new silver indium double phosphates and compare this structure with sodium analogs.

2. Experimental

2.1. Synthesis

The double phosphates of silver and indium $Ag_3In(PO_4)_2$ and β-$Ag_3In_2(PO_4)_3$ were obtained by solid state reaction from a stoichiometric mixtures of In_2O_3, $NH_4H_2PO_4$ and $AgNO_3$. The starting mixtures were grinded and dried at 300 °C for removing the volatile matter, sintered at 700 °C for 100 h in air and examined by powder X-ray diffraction. In the course of synthesis samples were grinded some times. Compounds obtained were single-phase well-crystallized white powders.

High temperature modification α-$Ag_3In_2(PO_4)_3$ was obtained after heating β-$Ag_3In_2(PO_4)_3$ at 900 °C for 50 h.

2.2. X-ray powder diffraction

Phase analysis was made at room temperature using a Siemens D500 powder diffractometer ($CuK_{\alpha1+\alpha2}$ radiation, $\lambda = 1.5406$ and 1.5443 Å, position sensitive detector (BRAUN)). The data were collected over a range of 5–60° (2θ) with a step of 0.02°, effective counting time was ca 1 s per step.

Powder diffraction data for indexing the X-ray patterns and structure refinement of $Ag_3In(PO_4)_2$ and β- and α-$Ag_3In_2(PO_4)_3$ were obtained at room temperature using a Siemens D500 powder diffractometer ($CuK_{\alpha1+\alpha2}$ radiation, $\lambda = 1.5406$ and 1.5443 Å, position sensitive detector (BRAUN)). The data were collected over a range of 5–100° (2θ) for $Ag_3In(PO_4)_2$ and β-$Ag_3In_2(PO_4)_3$ and 10–110° (2θ) for α-$Ag_3In_2(PO_4)_3$ with a step of 0.02°, effective counting time was ca. 10 s per step.

The indexing of $Ag_3In(PO_4)_2$ X-ray pattern was carried out in a monoclinic system ($a = 8.704(1)$Å; $b = 5.489(1)$Å; $c = 7.341(1)$Å; $\beta = 93.89(1)°$; $M_{20} = 56.7$; $F_{20} = 82.6$). Systematic-existing conditions were consistent with non-centrosymmetric ($C2$ (no. 5), Cm (no. 8)) and centrosymmetric ($C2/m$ (no. 12)) space groups. The choice of the space group ($C2/m$) was determined by second harmonic generation (SHG) ($I_{2\omega}/I_{2\omega(SiO_2)} = 0.1$).

The analysis of the reflex positions in the X-ray pattern of the sample α- and β-$Ag_3In_2(PO_4)_2$ has shown that both compounds are isostructural to the Na-analogs [13,22]. The cell parameters were determined by indexing the X-ray pattern of α- and β-$Ag_3In_2(PO_4)_2$: α-phase—sp.gr. R-3c; $a = 8.993(1)$Å, $c = 22.717(1)$Å, $M_{20} = 43.4$, $F_{20} = 52.1$; β-phase—sp.gr. $C2/c$; $a = 12.642(1)$Å, $b = 12.858(1)$Å, $c = 6.599(1)$Å, $\beta = 113.86(1)°$, $M_{20} = 23.4$, $F_{30} = 44.1$.

The choice of the centrosymmetric space groups in both cases was determined by SHG ($I_{2\omega}/I_{2\omega(SiO_2)} = 0.2$) and space groups of structure analogs.

2.3. Structure determination

All calculations were carried out with an updated MRIA program [23]. The split-type Pseudo-Voigt peak profile function was used for X-ray powder data. The background was approximated by a Chebyshev polynomial. Structure analogs for $Ag_3In(PO_4)_2$ are not found. 207F^2 values extracted from the diffraction pattern using the full-pattern-decomposition (FPD) procedure of MRIA package program were used as input for the Patterson methods routine of the DIRDIF96 program [24]. As the results position of all atoms were determined. For refinement α- and β-$Ag_3In_2(PO_4)_3$ structures were used atomic parameters of α- and β-$Na_3In_2(PO_4)_3$.

The X-ray patterns of the samples $Ag_3In(PO_4)_2$ showed preferred orientation. March–Dollase [25] and symmetrized harmonics expansion [26,27] texture formalisms were used while processing X-ray pattern. In first case texture parameter $\boldsymbol{r}$ was 1.14 (2) (preferred orientation vectors—[0 0 1]; $R_{WP} = 11.81\%$, $R_P = 7.94\%$, $R_{Bragg} = 14.82\%$). In second one six parameters varied and the greatest correction was observed for $00l$-series (1.197) and the lowest correction was observed for $0k0$-series (0.894).

In the refinement process some constraints were introduced. Isotropic atomic displacement parameters for oxygen atoms of $P(1)O_4$ and $P(2)O_4$ β-$Ag_3In_2(PO_4)_3$ were equal.

At first refinement α-$Ag_3In_2(PO_4)_3$ with atoms of silver in special positions as in NASICON structures was conducted and isotropic atomic displacement parameters were $-3.4(4)$ and $6.3(3)$ Å^2 for Ag(1) and Ag(2) correspondingly. Then Ag(1) was shifted in 36f-position the B(Ag(1)) and B(Ag(2)) were 5.24 Å^2 and 5.96 Å^2 ($R_p = 8.73\%$; $R_{wp} = 11.62\%$). In the end after constraint of silver's isotropic parameters there are B(Ag(1)) = B(Ag(2)) = 5.37 Å^2 and $R_p = 7.30\%$; $R_{wp} = 9.91\%$.

Full profile refinement was made by the Rietveld method procedure (RR). Details for the final refinements are given in Table 1, atomic coordinates in Table 2 and main distances in Tables 3–5. Figs. 1–3 show the Rietveld plot with a good agreement between the observed and the calculated patterns.

2.4. Second harmonic generation

The SHG response of synthesized phosphates powders was measured in the reflection mode. A Q-switch pulsed Nd:YAG laser operating at 1064 nm with a 6.25 Hz repetition rate and a 12 ns pulse width was used as radiation source. The average power incident on the reflector was 0.5 MW. Powdered crystalline SiO_2 was used as a standard sample. In all cases means of SHG is lower 0.5 and not exclude centrosymmetric space groups. The

Table 1
Experimental details

Compound	$Ag_3In(PO_4)_2$	β-$Ag_3In_2(PO_4)_3$	α-$Ag_3In_2(PO_4)_3$
Space group, Z	$C2/m$, 2	$C2/c$, 4	R-3c, 6
Interval 2Θ (°)	5–100	5–100	10–110
Step	0.02	0.02	0.02
I_{max}	43,572	25,454	59,303
Lattice parameters			
a (Å)	8.7037(1)	12.6305(1)	8.9943(1)
b (Å)	5.4885(1)	12.8549(1)	
c (Å)	7.3404(1)	6.5989(1)	22.7134(1)
β (°)	93.897(1)	113.842(1)	
V (Å^3)	349.84(1)	979.99(1)	1591.28(1)
Refinement parameters			
Structural	21	31	20
Another	37	31	31
Agreement factors			
R_p, R_{bragg}, R_{wp} (%)	6.47, 11.82, 8.54	5.67, 9.26, 6.40	7.30, 10.57, 9.91

Table 2
Atomic parameters.

Atom	Wyckoff position	x	y	z	B
$Ag_3In(PO_4)_2$					
In	2a	0	0	0	1.97(1)
Ag1	4i	0.1723(1)	0.5	−0.3188(1)	2.61(1)
Ag2	2c	0.5	0.5	0.5	3.47(1)
P	4i	0.1585(2)	0.5	0.2080(2)	3.16(2)
O1	4i	0.2536(4)	0.5	0.3927(3)	4.74(2)
O2	4i	0.2633(4)	0.5	0.0507(4)	2.61(2)
O3	8j	0.0543(3)	0.2819(4)	0.2073(3)	3.95(2)
β-$Ag_3In_2(PO_4)_3$					
In	8f	0.2289(1)	0.1561(1)	0.1539(1)	1.34(1)
P1	8f	0.2403(2)	−0.1021(2)	0.1354(4)	1.26(1)
P2	4e	0.0000	0.2690(2)	0.7500	0.39(1)
O1	8f	0.3625(2)	−0.0774(3)	0.1629(4)	2.45(3)
O2	8f	0.2465(3)	−0.1701(3)	0.3336(4)	2.45(3)
O3	8f	0.1739(3)	−0.0026(2)	0.1321(4)	2.45(3)
O4	8f	0.1752(3)	−0.1623(3)	−0.0786(4)	2.45(3)
O5	8f	0.0506(4)	0.1935(3)	0.9406(4)	1.66(4)
O6	8f	0.0909(4)	0.3365(3)	0.722(1)	1.66(4)
Ag1	4e	0.0000	0.2784(1)	0.2500	2.05(1)
Ag2	4e	0.0000	−0.0031(1)	0.7500	2.68(1)
Ag3	4b	0.5000	0.0000	0.5000	2.29(1)
α-$Ag_3In_2(PO_4)_3$					
In	12c	0	0	0.14994(2)	1.66(1)
P1	18e	0.2916(2)	0	0.25	1.42(2)
O1	36f	0.1850(3)	−0.0325(3)	0.1950(1)	3.40(2)
O2	36f	0.3147(3)	−0.1563(3)	0.2536(1)	2.05(2)
Ag1	36f[a]	0.0684(4)	0.016(1)	−0.0003(4)	5.37(4)
Ag2	18e[b]	0.6462(1)	0	0.25	5.37(4)

[a] Occupancy 0.167.

[b] Occupancy 0.667.

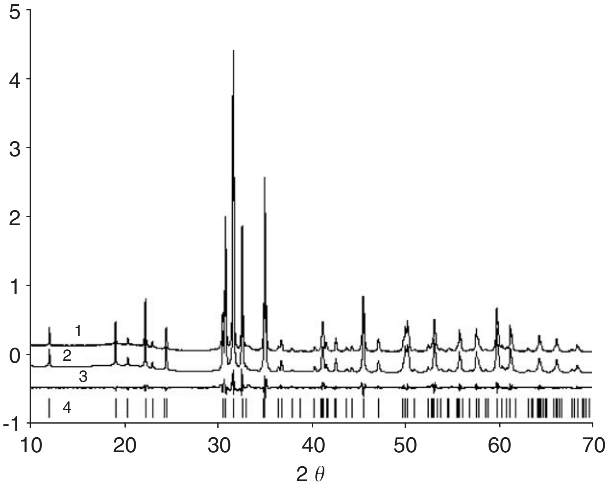

Fig. 1. Portion of the Rietveld refinement profiles for $Ag_3In(PO_4)_2$; 1—calculated, 2—observed, 3—difference X-ray powder diffraction patterns, and 4—Bragg reflections.

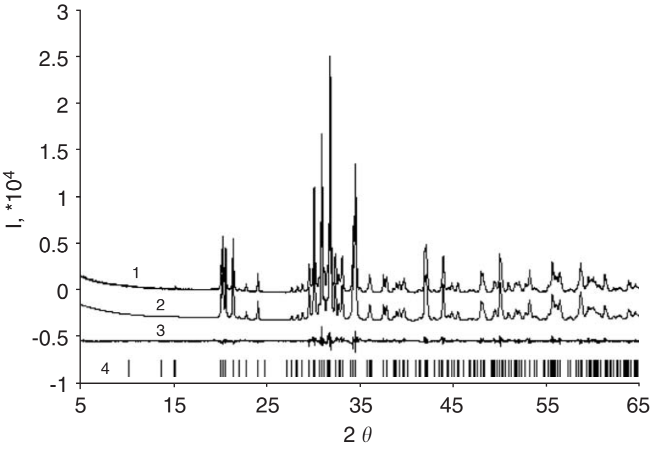

Fig. 2. Portion of the Rietveld refinement profiles for β-$Ag_3In_2(PO_4)_3$; 1—calculated, 2—observed, 3—difference X-ray powder diffraction patterns, and 4—Bragg reflections.

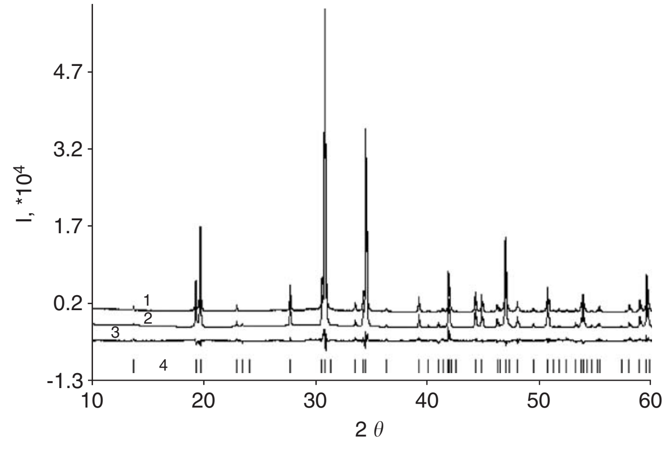

Fig. 3. Portion of the Rietveld refinement profiles for α-$Ag_3In_2(PO_4)_3$; 1—calculated, 2—observed, 3—difference X-ray powder diffraction patterns, and 4—Bragg reflections.

powder samples of all investigated compounds showed SHG responses, $I_{2\omega}/I_{2\omega}$ (SiO_2) < 0.3. This responses are indicative of a centrosymmetric space group.

2.5. *Thermogravimetric analysis*

The thermogravimetric analysis (TGA) (DTA, TG, DTG) was performed using derivatographs Q1500 and NETZSCH STA 449C. Sample masses were of 100–150 mg (Q1500) and 10–20 mg (NETZSCH STA 449C). The compounds involved were heated from 20 to 1000 °C at 10 °C/min in air.

It is stated by the thermal analyses that the β-$Ag_3In_2(PO_4)_3 \rightarrow \alpha$-$Ag_3In_2(PO_4)_3$ transition occurs irreversibly at 812 °C. The compound $Ag_3In(PO_4)_2$ is stable up to 753 °C. Above this temperature, this phase is decomposed providing silver orthophosphate Ag_3PO_4 and α-$Ag_3In_2(PO_4)_3$.

3. Results and discussion

The main building blocks of structure $Ag_3In(PO_4)_2$ are InO_6-octahedra and PO_4-tetrahedra. Indium atoms are placed in center of slightly strained octahedron InO_6. In–O distances are equal to 2.12 and 2.19 Å in the octahedron (Table 3). Octahedra joined by PO_4-tetrahedra form untied infinite layers. Average distance P–O in PO_4-tetrahedra (1.516 Å) is close to the characteristic distance in phosphates (1.52 Å).

Table 3
Selected interatomic distances (Å) and angles (°) in structure

$Ag_3In(PO_4)_2$		β-$Ag_3In_2(PO_4)_3$		α-$Ag_3In_2(PO_4)_3$	
Distances In–O					
In–O2 × 2	2.118(1)	In–O2	**2.253(1)**	**In–O1 × 3**	2.095(1)
In–O3 × 4	2.199(1)	In–O2	2.220(1)	In–O2 × 3	2.208(1)
⟨In–O⟩	**2.152**	In–O3	2.141(1)	**⟨In–O⟩**	**2.152**
		In–O4	2.133(1)		
		In–O5	2.173(1)		
		In–O6	2.086(1)		
		⟨In–O⟩	**2.168**		
Distances P–O					
P–O1	1.540(1)	P1—O1	1.513(1)	P–O1 × 2	1.512(1)
P–O2	1.519(1)	P1—O2	1.549(1)	P–O2 × 2	1.523(1)
P–O3 × 2	1.502(1)	P1—O3	1.525(1)	**⟨P–O⟩**	**1.517**
⟨P–O⟩	**1.516**	P1—O4	1.527(1)		
		⟨P1–O⟩	**1.529**		
		P2—O5 × 2	1.511(1)		
		P2—O6 × 2	1.508(1)		
		⟨P2–O⟩	**1.510**		
Distances Ag–O					
Ag1–O1	2.278(1)	Ag1—O1 × 2	**2.445(1)**	Ag1—O2	**2.719(1)**
Ag1–O1 × 2	2.879(1)	Ag1—O4 × 2	2.526(1)	Ag1—O2	2.288(1)
Ag1—O2	2.773(1)	Ag1—O5 × 2	2.612(1)	Ag1—O2	2.900(1)
Ag1–O3 × 2	2.492(1)	Ag1—O6 × 2	2.948(1)	Ag1—O2	2.586(1)
Ag1–O3 × 2	2.909(1)	**⟨Ag1–O⟩**	**2.633**	Ag1—O2	2.973(1)
⟨Ag–O⟩	**2.641**			Ag1—O2	2.381(1)
				⟨Ag–O⟩	**2.641**
Ag2–O1 × 2	2.234(1)	Ag2—O3 × 2	2.589(1)	Ag2–O2 × 2	2.585(1)
Ag2–O3 × 4	2.715(1)	Ag2—O3 × 2	2.611(1)	Ag2—O2 × 2	2.479(1)
⟨Ag–O⟩	**2.658**	Ag2—O4 × 2	2.888(1)	Ag2—O1 × 2	2.806(1)
		Ag2—O5 × 2	2.780(1)	Ag2—O1 × 2	2.765(1)
		⟨Ag2–O⟩	**2.717**	**⟨Ag–O⟩**	**2.658**
		Ag3—O1 × 2	2.583(1)		
		Ag3—O1 × 2	2.415(1)		
		Ag3—O6 × 2	2.554(1)		
		⟨Ag3–O⟩	**2.517**		
Angles					
∠(O2–In–O2)	180.00	∠(O2–In–O6)	81.73(1)	∠(O1–In–O1) × 3	98.13(1)
∠(O2–In–O3) × 4	92.54(1)	∠(O3–In–O4)	83.58(1)	∠(O1–In–O2) × 3	90.86(1)
∠(O2–In–O3) × 4	87.46(1)	∠(O3–In–O5)	86.80(1)	∠(O1–In–O2) × 3	87.40(1)
∠(O3–In–O3) × 2	89.44(1)	∠(O3–In–O6)	110.04(1)	∠(O1–In–O2) × 3	168.63(1)
∠(O3–In–O3) × 2	90.56(1)	∠(O4–In–O5)	86.26(1)	∠(O2–In–O2) × 3	82.57(1)

Table 3 (*continued*)

$Ag_3In(PO_4)_2$		β-$Ag_3In_2(PO_4)_3$		α-$Ag_3In_2(PO_4)_3$	
∠(O3–In–O3) × 2	180.00	∠(O4–In–O6)	109.60(1)		
		∠(O5–In–O6)	157.60(1)		
		∠(O2–In–O2)	83.63(1)		
		∠(O2–In–O3)	99.67(1)		
		∠(O2–In–O3)	169.64(1)		
		∠(O2–In–O4)			
		∠(O2–In–O4)	91.03(1)		
		∠(O2–In–O5)	166.53(1)		
		∠(O2–In–O5)	80.89(1)		
		∠(O2–In–O6)	84.02(1)		
			80.09(1)		
∠(O1–P1–O2)	110.77(1)	∠(O1–P1–O2)	108.44(1)	∠(O1–P1–O1)	114.96(1)
∠(O1–P1–O3) × 2	106.94(1)	∠(O1–P1–O3)	110.74(1)	∠(O1–P1–O2) × 2	103.42(1)
∠(O2–P1–O3) × 2	113.02(1)	∠(O1–P1–O4)	111.05(1)	∠(O1–P1–O2) × 2	114.27(1)
∠(O3–P1–O3)	105.72(1)	∠(O2–P1–O3)	108.98(1)	∠(O2–P1–O2)	106.53(1)
		∠(O2–P1–O4)	108.64(1)		
		∠(O3–P1–O4)	108.94(1)		
		∠(O5–P2–O5)	100.06(1)		
		∠(O5–P2–O6) × 2	110.79(1)		
		∠(O5–P2–O6) × 2	112.59(1)		
		∠(O6–P2–O6)	109.76(1)		

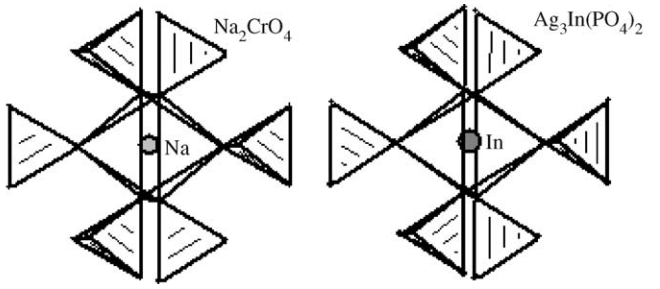

Fig. 4. Tetrahedra arrangement in the structures Na_2CrO_4 and $Ag_3In(PO_4)_2$.

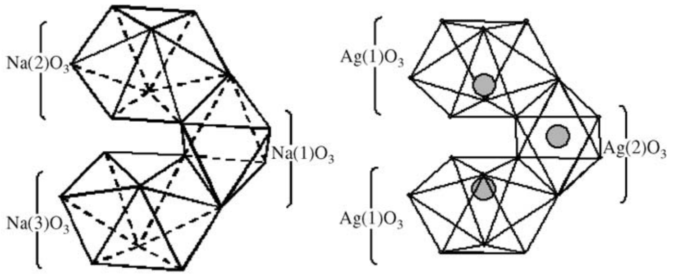

Fig. 5. NaO_x- and AgO_x-polyhedra in $Na_3In(PO_4)_2$ and $Ag_3In(PO_4)_2$ correspondingly.

Silver atoms are situated between layers in two positions 4*i* and 2*c*. Coordination numbers of silver atoms is equal 6 (Ag(2)) and 8 (Ag(1)). Polyhedra $Ag(1)O_8$ and $Ag(2)O_6$ are strained very strong. They are joined by shared edge O(1)–O(3) with each other.

Structure of double phosphate $Ag_3In(PO_4)_2$ as α-$Na_3In(PO_4)_2$ is similar with Na_2CrO_4 structure (Fig. 4). Comparison of $Ag_3In(PO_4)_2$ and Na_2CrO_4 shows that In^{3+}-cation occupies Na(2)-position. On going from Na_2CrO_4 structure to $Ag_3In(PO_4)_2$ structure the position of Na(1) is transformed to two nonequivalent positions occupied by Ag^+-cations.

The main difference between $Ag_3In(PO_4)_2$ and α-$Na_3In(PO_4)_2$ [5] structures consists of a number of monovalent cations positions (Fig. 5). Going from $Ag_3In(PO_4)_2$ (sp. gr. $C2/m$) to α-$Na_3In(PO_4)_2$ (sp. gr. $P2_1/m$), 4*i*-position occupied by Ag(1) breaks into two 2*e* equivalent positions occupied by Na(2) and Na(3). Polyhedra shape is equal in both cases. $Ag_3In(PO_4)_2$ has no another modification.

The structure of β-$Ag_3In_2(PO_4)_3$ is shown in Fig. 6a. Two octahedra InO_6 are connected by a shared edge in In_2O_{10} dimers (bioctahedra) (Fig. 6b). Ten atoms of oxygen belong to eight PO_4-tetrahedra. Two of ten PO_4 groups in the dimer are bridging and fix the distances between the vertices of the octahedra. As a result, this distance In···In in the dimer must be approximately equal to 3.0 Å. Due to repulsion between the cations, this distance increases to 3.35 Å.

The atoms of silver have a coordination sphere from eight and six oxygen atoms (Fig. 6a) in this structure. The octahedron $Ag(3)O_6$ is weakly distorted. Two coordination spheres of Ag(1) and Ag(2) can be isolated. The internal ones contain four oxygen atoms on distance 2.445 and 2.526 Å (Ag(1)), 2.589 and 2.611 Å (Ag(2)) in the planar position and the external ones contain four oxygen atoms on distance 2.612 and 2.948 Å (Ag(1)), 2.888 and 2.780 Å (Ag(2)).

Structural formula of β-$Ag_3In_2(PO_4)_3$ is $[X(2)][X(1)][M(1)][M(2)]_2(PO_4)_3$ as a formula of alluaudite-like

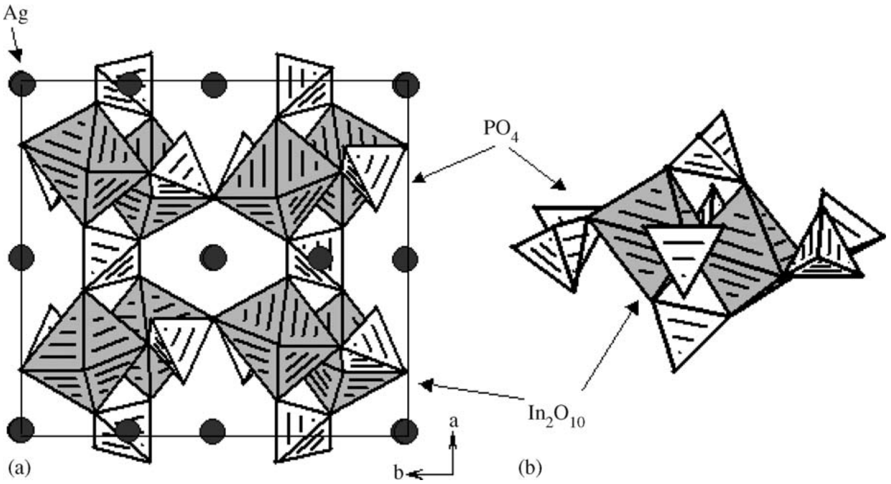

Fig. 6. Projection of β-$Ag_3In_2(PO_4)_3$ structure along *c*-axis (a) and dimer block In_2O_{10} (b).

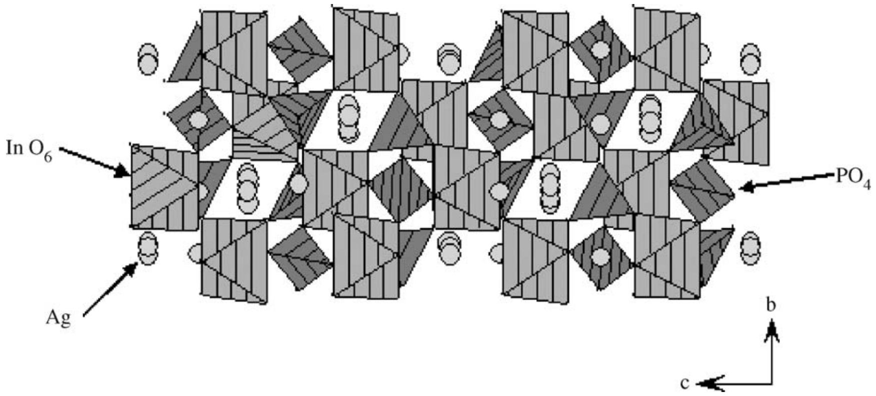

Fig. 7. Projection of α-$Ag_3In_2(PO_4)_3$ structure along *a*-axis.

structure phosphates (for example $AgCaIn_2(PO_4)_3$ [21], $NaCaMn^{2+}\ Fe_2^{2+}\ (PO_4)_3$ [28]). In our structure *X*(1) (0.5, 0, 0) position is occupied by Ag(3) atoms while the *X*(2) (0, 0, 0) position is vacant. Otherwise the Ag(2) atoms shifted from the *X*(2) position on ±0.25 along *z*-axis are situated in the tunnels (0, 0, *z*) like the displacement this position in the structure $NaMn_3(PO_4)(HPO_4)_2$ [29]. The Ag(1) and In occupy *M*(1) and *M*(2) positions forming infinite chains *M*(1)–*M*(2)–*M*(2) including In_2O_{10} dimers. These chains are connected by phosphate tetrahedra into layers and a three-dimensional framework.

Three-dimension framework of structure α-$Ag_3In_2(PO_4)_3$ is built of InO_6 octahedra connected by PO_4 tetrahedra (Fig. 7). Coordination environment of indium atoms is distorted octahedra with distances In–O 2.095 and 2.208 Å (Table 3).

The cavities in the framework are occupied by silver cations. The frameworks of the structures are penetrated by channels in which the silver atoms are situated. Coordination numbers of silver are eight and six. Octahedron $Ag(1)O_6$ is strongly distorted. Distances Ag–O are layered in wide interval values (from 2.288 to 2.973 Å). On the other hand, average distance Ag–O (2.658 Å) in $Ag(2)O_8$-polyhedra is close to calculated distance from ionic radii silver and oxygen ($r_{\mathrm{VIII}}(Ag^+) + r(O^{2-}) = 2.65$ Å) [19].

This modification of $Ag_3In_2(PO_4)_3$, like compounds $Na_3M_2^{\mathrm{III}}(PO_4)_3$ (M^{III} = In, Sc, Cr, Fe) [1,30] has NASICON-like structure. The factors that determine existing conditions of this structure type are possibility of M^{III}-cations are situated in octahedra and presence small monovalent elements in the structure. Structure is based on framework $\{[In_2(PO_4)_3]\}_{3\infty}$, as other NASICON-like structures. There are channels of two types, I and II, extended along the *b*-axis of the unit cell in the framework of the structure. The channels of type III are perpendicular to the channels I and II and intersect these channels. The large cavities in these channels are occupied statistically by silver atoms. This compound is distinguished from other ones having similar structures by position of Ag(1). The atom is placed on position (36*f*) with occupancy 1/6 near the special position 6*b*, in

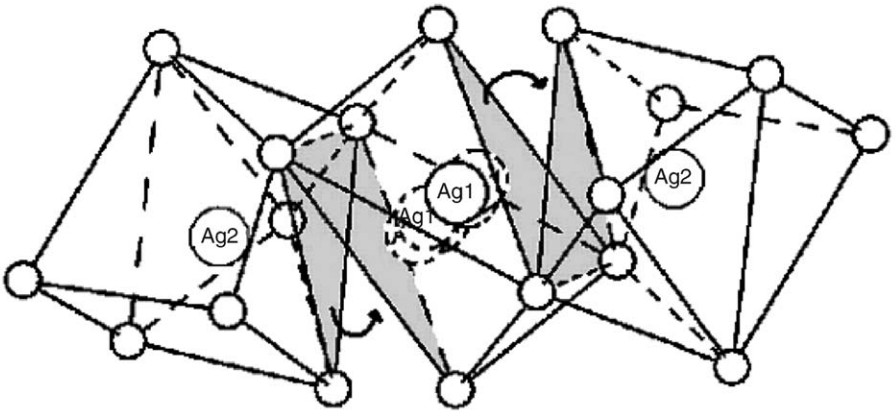

Fig. 8. Polyhedra of silver cations in structures α-$Ag_3In_2(PO_4)_3$ (Ag(1)–36*f*; Ag(2)–18*e*). Arrows show possible cation move.

which monovalent atoms of NASICON-like structure is located (Fig. 8). Proportion of edges ($r \sim 1$ Å) is sufficient for moving silver atoms through it, i.e. for ionic conductivity. The possible path of silver ions is shown by arrows on Fig. 8.

The analysis of the polyhedra in the crystal structure of β-$Ag_3In_2(PO_4)_3$ leads one to the conclusion that the complete occupancy of the *M*(2) position by a double- or triple-charged cation is a necessary condition for crystallization of double phosphates in the alluaudite structural type. It should be noted that the ionic radius of the cation in the dimer [*M*(2) position] must be in the strictly specified range $0.76 \leqslant r \leqslant 0.78$ Å. The radii r of the Fe^{2+} and In^{3+} cations fall within this range. The fact is that the occurrence of alluaudite-like structures is determined by the size of the PO_4 tetrahedron. The larger or smaller size of the cation as compared to In^{3+} ($r<0.76$ and $r>0.78$ Å) will lead to destruction of the dimer as the structural block, which is confirmed by the lack of information on alluaudite-like phases with composition $M^{I}_3M^{III}_2(PO_4)_3$ where M^{III} = rare-earth elements, Sc, Fe, Cr.

From the crystal-chemical viewpoint, the transformation of the alluaudite-like β-phase into the NASICON-like α phase (which was established from the analysis of the structures of both modifications of $Ag_3In_2(PO_4)_3$) involves the radical rearrangement of the atoms. It was demonstrated that the transformation from the β-phase to the phase is accompanied by an increase in the distance between the indium atoms, destruction of the In_2O_{10} dimers and formation of the isolated InO_6 octahedra. This rearrangement leads to an increase in 'porosity' [$\Delta(V/Z)_{\beta\rightarrow\alpha} = 8.25\%$] of the crystal structure due to the formation of rather large channels, which are statistically occupied by alkali-metal cations.

So silver–indium double phosphates $Ag_3In(PO_4)_2$ and $Ag_3In_2(PO_4)_3$ bear similarities to Na-analogs: both modifications of $Ag_3In_2(PO_4)_3$ are isostructural to α- and β-$Na_3In_2(PO_4)_3$ and $Ag_3In(PO_4)_2$ structure is close with α-$Na_3In(PO_4)_2$ structure.

Acknowledgments

Authors thank Dr. S. Yu. Stefanovich (Moscow State University, Russia) for SHG measurements and Dr. Ev. Al. Gudilin (Moscow State University, Russia) for TGA measurements.

Reference

[1] B.I. Lazoryak, Uspekhi. Khim. (Russ.) 65 (1996) 307.
[2] S.U. Stefanovich, V.B. Kalinin, Solid State Phys. (Russ.) 23 (1981) 3509.
[3] M. Vlasse, C. Parent, R. Salmon, G. Le Flem, P. Hagenmuller, J. Solid State Chem. 35 (1980) 318.
[4] R. Salmon, C. Parent, M. Vlasse, G. Le Flem, Mater. Res. Bull. 13 (1978) 439.
[5] M.G. Zhizhin, V.A. Morozov, L.N. Komissarova, B.I. Lazoryak, J. Solid State Chem. 149 (2000) 99.
[6] F. Mazzi, L. Ungaretti, Neues Jahrbuch fuer Mineral. (Band = Jahr). 2 (1994) 49.
[7] R. Salmon, C. Parent, M. Vlasse, G. Le Flem, Mater. Res. Bull. 14 (1979) 85.
[8] V.A. Morozov, B.I. Lazoryak, A.P. Malakho, K.V. Pokholok, S.N. Polyakov, T.P. Terekhina, J. Solid State Chem. 160 (2) (2001) 377.
[9] Q.D. Tran, S. Hamdoune, Acta Crystallogr. Ser. C 43 (1987) 397.
[10] C. Masquelier, C. Wurm, J. Rodríguez-Carvajal, J. Gaubicher, L. Nazar, Chem. Mater. 12 (2) (2000) 525.
[11] T. Suzuki, K. Yoshida, K. Uematsu, T. Kodama, K. Toda, Z.-G. Ye, M. Ohashi, M. Sato, Solid State Ion. 113 (1998) 89.
[12] E.A. Genkina, L.A. Mudaryan, B.A. Maximov, B.A. Merinov, S.E. Sigarev, Crystallografya (Russ.) 32 (1987) 74.
[13] K.-H. Lii, J. Ye, J. Solid State Chem. 131 (1997) 131.
[14] B.I. Lazoryak, S.U. Stefanovich, V.B. Kalinin, Docl. Acad. Nauk SSSR (Russ.) 250 (1980) 861.
[15] E.A. Genkina, V.B. Kalinin, B.A. Maximov, A.M. Golubev, Crystallografya (Russ.) 36 (1991) 1126.
[16] N. Fanjat, J.L. Soubeyroux, J. Magn. Magn. Mater. 104 (1992) 933.
[17] J. Winand, A. Rulmont, P. Tarte, J. Mater. Sci. 25 (1990) 4008.
[18] V.B. Kalinin, V.A. Efremov, Crystallografya (Russ.) 23 (1978) 703.
[19] R.D. Shannon, Acta Cryst. A 32 (1976) 751.
[20] L.O. Atovmyan, V.V. Tkachev, J. Coord. Chem. (Russ.) 21 (7) (1995) 562.
[21] Powder Diffraction File Card 46-0532, JCPDS, International Center of Diffraction Data, 1601 Park Lane, Swartmore, PA 19081.

[22] A.K. Ivanov-Shits, S.E. Sigarev, Zh. Phiz. Tver. Tela (Russ.) 28 (1986) 3528.

[23] V.B. Zlokazov, V.V. Chernyshev, J. Appl. Crystallogr. 25 (1992) 447.

[24] P.T. Beurskens, G. Beurskens, W.P. Bosman, R. de Gelder, S. Garcia-Granda, R.O. Gould, R. Israel, J.M.M. Smits, The DIRDIF-96 Program System, Crystallography Laboratory, University of Nijmegen, The Netherlands, 1996.

[25] W.A. Dollase, J. Appl. Crystallogr. 19 (1986) 267.

[26] M. Ahtee, M. Nurmela, P. Suortti, M. Järvinen, J. Appl. Crystallogr. 22 (1989) 261.

[27] M. Järvinen, J. Appl. Crystallogr. 26 (1993) 525.

[28] D.J. Fisher, Am. Mineral. 40 (1955) 1100.

[29] S. Khorari, A. Rulmont, R. Cahay, P. Tarte, J. Solid State Chem. 118 (1995) 267.

[30] L.N. Komissarova, M.G. Zhizhin, A.A. Filaretov, Uspekhi. Khim. (Russ.) 71 (2002) 707.